

Structure of glassy lithium sulfate films sputtered in nitrogen: Insight from Raman spectroscopy and *ab initio* calculations

Christian R. Müller,¹ Patrik Johansson,² Maths Karlsson,² Philipp Maass,^{1,*} and Aleksandar Matic²

¹*Institut für Physik, Technische Universität Ilmenau, 98684 Ilmenau, Germany*

²*Department of Applied Physics, Chalmers University of Technology, 41296 Göteborg, Sweden*

(Received 18 June 2007; revised manuscript received 6 December 2007; published 12 March 2008)

Raman spectra of thin solid electrolyte films obtained by sputtering a Li_2SO_4 target in nitrogen plasma are measured and compared to *ab initio* electronic structure calculations for clusters composed of 28 atoms. Agreement between measured and calculated spectra is obtained only when some oxygen atoms are replaced by nitrogen atoms and when these nitrogen atoms form bonds with each other. This suggests that the incorporation of nitrogen during the sputtering process leads to structures in the film, which prevent crystallization of these thin film salt glasses.

DOI: [10.1103/PhysRevB.77.094116](https://doi.org/10.1103/PhysRevB.77.094116)

PACS number(s): 78.55.Qr, 61.43.Fs, 82.45.Gj

I. INTRODUCTION

Glassy thin film electrolytes are materials of considerable technological interest. They are used in the design of modern solid state batteries, electrochemical sensors, supercapacitors, and electrochromic devices. Most of the materials nowadays are fabricated using the sol-gel methods, but different possibilities are currently explored by using sputtering techniques. Examples are thin films produced by sputtering a $0.75\text{Li}_2\text{O}-0.25\text{P}_2\text{O}_5$ target in a nitrogen plasma (LIPON¹), which show ionic conductivities of about $3 \times 10^{-6} \Omega^{-1} \text{cm}^{-1}$. This material has been successfully used in microbatteries² and electrochromic systems.³ Through the mixed network former effect, the ionic conductivity could be further increased to about $9 \times 10^{-6} \Omega^{-1} \text{cm}^{-1}$ by taking a $0.75\text{Li}_2\text{O}-0.25[0.2\text{SiO}_2-0.8\text{P}_2\text{O}_5]$ target.⁴

The sputtering technique is, in particular, interesting, since it extends the glass forming range. This has recently been observed in the ternary $\text{Li}_2\text{O}-\text{B}_2\text{O}_3-\text{Li}_2\text{SO}_4$ systems,⁵ where the sulfate content could be increased to amounts that would lead to crystallization when preparing glass by melt quenching. In fact, the borate component can be fully eliminated by sputtering a Li_2SO_4 target in a nitrogen containing plasma, leading to an amorphous material referred to as LISON.⁶ With respect to the target material, one could speak of a “salt glass.” Similar stabilization effects of nitrogen during sputtering have been observed also in quite different thin film materials, such as, for example, diamondlike carbon films^{7–10} and iron or Permalloy ($\text{Ni}_{80}\text{Fe}_{20}$) films.¹¹ In the carbon thin films, it is believed that the incorporation of nitrogen atoms leads to a buckling of the graphite planes and an associated formation of sp^3 hybridized carbon atoms, which act as cross linkers between the planes. In the iron and nickel-iron films, the nitrogen is suggested to occupy interstitial sites, leading to an expansion of the unit cells and a subsequent suppression of long-range crystalline order.

For the sputtering of the Li_2SO_4 target, it is found that sputtering in an argon plasma does not lead to an amorphous film, indicating that nitrogen plays a crucial role in the glass forming ability. Indeed, it was shown that nitrogen is partly incorporated into the material⁶ with a sulfur to nitrogen ratio of about 2:1. At present, it is not clear how the structure of

these salt glasses is built up, in particular, in which way the incorporation of nitrogen takes place and how this leads to a stabilization of the amorphous structure.

The aim of this work is to get insight into the structural arrangements of this glass system. In particular, it is of interest how the nitrogen is incorporated into the structure and how this is related to the increased stability of the material toward crystallization. To this end, we study LISON films by Raman spectroscopy and compare the vibrational spectra with predictions from *ab initio* electronic structure calculations based on density functional theory. Calculations have been performed for pure Li_2SO_4 clusters and nitrogen doped Li_2SO_4 clusters.

II. EXPERIMENT

The Raman experiments were performed at room temperature in an argon atmosphere using a micro-Raman setup with an argon-krypton laser tuned to the 514 nm line as the excitation source. With this experimental setup, we have a depth resolution of 14 μm . The powers at the sample were 21 mW for the depolarized configuration (perpendicular direction of polarization of the incoming beam with respect to the polarizer in front of the detector) and 7 mW for the polarized configuration. The integration time of a single measurement was 300 s. The analysis of the spectrum is based on the median of 27 spectra. Measurements on different spots of the sample gave the same spectrum, showing that the film was homogeneous.

The LISON film had a thickness of 4 μm and was prepared by sputtering a Li_2SO_4 target in nitrogen plasma at pressure of 1 Pa.¹² Due to the rather strong Raman response of the silicon substrate and the small thickness of the film, the measured spectra are dominated by the silicon signal. In order to obtain the response of the film, a reference spectrum from a clean silicon substrate was subtracted. In this procedure, it was important to ensure that the substrate had the same orientation with respect to the incident polarization, wherefore we made use of the polarization dependence of the intensity of the 521 cm^{-1} Raman line of silicon.

III. AB INITIO CALCULATIONS

We performed electronic structure calculations for Li_2SO_4 clusters with 28 atoms (four Li_2SO_4 units). Start configurations were created based on the conception that the lithium sulfate salt glass consists of intact SO_4 units with lithium atoms in between. Using the GAUSSVIEW3.0 program,¹⁴ we constructed SO_4 tetrahedra with random orientation and added lithium atoms under the constraint of minimum interatomic distance of 1.6 Å.

The initial configurations were geometry optimized using the GAUSSIAN03 suite of quantum chemistry programs¹⁵ (for the theoretical background underlying the methods, see Ref. 16). First, the semiempirical PM3 method was applied, followed by a Hartree-Fock calculation with the 6-31G* basis set. These calculations took about 200 CPU hours and 200 iterations. For the final optimization using the hybrid density functional B3LYP and the same basis set, only a few iterations were needed.

In order to monitor the influence of nitrogen, we replaced oxygen atoms with nitrogen atoms in the optimized Li_2SO_4 cluster configurations. These modified clusters were again optimized by employing the Hartree-Fock and B3LYP with the 6-31G* basis set.

From the second and third order derivatives of the potential energy surface (PES) at the minima found for the optimized configurations, we calculated the Raman spectra. It is clear that the amorphous film will exhibit a large number of local structures corresponding to different minima of the PES. By optimizing different starting configurations, it is possible to scan a part of the PES and to find minima, whose associated clusters are good representatives of the local structures of the LISON film. This is evaluated by comparing the calculated vibrational spectra with the experimental ones.

IV. EXPERIMENTAL RESULTS

Figure 1 shows (a) the polarized and (b) depolarized Raman spectra for the LISON film. The bare silicon (dashed line) and the sample spectrum (film plus substrate, solid line) are shown in the insets of Figs. 1(a) and 1(b). The bare silicon spectrum was scaled to fit the characteristics between 250 and 350 cm^{-1} . The most pronounced feature of the resulting difference spectra in Figs. 1(a) and 1(b) is a main band between 850 and 1035 cm^{-1} . A second weaker band is found at 1225 cm^{-1} with a shoulder at slightly lower frequencies, around 1150 cm^{-1} , in the polarized spectrum in Fig. 1(a). In addition, two more bands can be discerned at 415 and 645 cm^{-1} , in particular, in the case of the polarized spectrum, where the intense silicon mode at 521 cm^{-1} is absent and does not hamper the subtraction procedure. The intensity gap between 440 and 500 cm^{-1} in the depolarized spectrum results from the fact that, in order to resolve the weak difference signals, the integration time had to be sufficiently large. As a consequence, the intensity of the silicon mode at 521 cm^{-1} present in the depolarized spectrum [see the inset of Fig. 1(b)] saturates the detector in this spectral region.

In order to assign the bands originating from the LISON film in the difference spectra in Fig. 1, we compare the re-

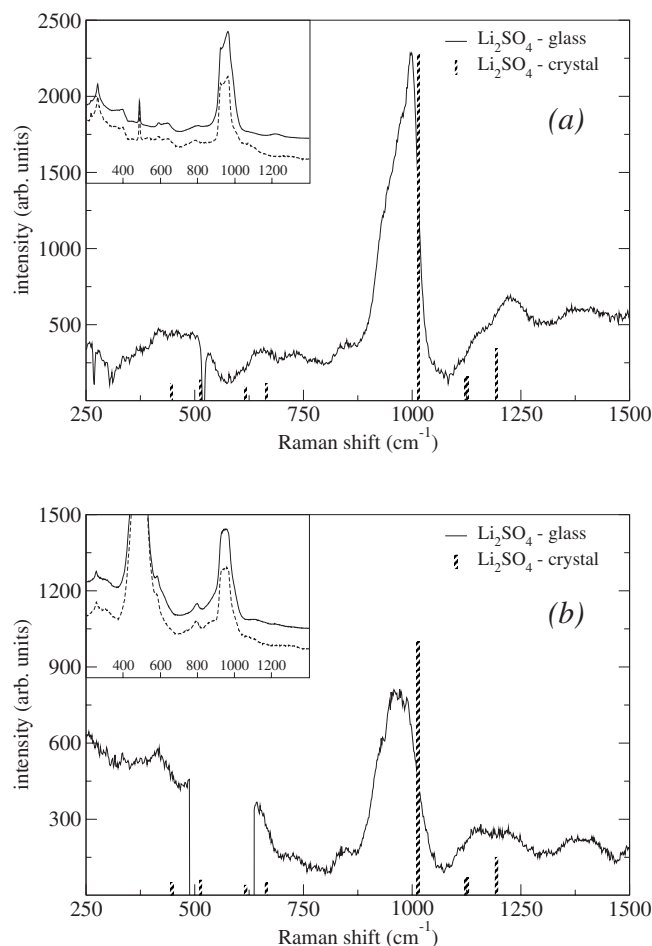


FIG. 1. (a) Polarized and (b) depolarized difference Raman spectra of LISON films on a silicon substrate. The difference signal is obtained by subtracting the spectrum of a bare silicon substrate from the spectrum of the sample. The insets show the raw data from the sample and the substrate (dashed lines, silicon; solid lines, LI-SO₄ film sample). The spectra have been offset for clarity.

sults to the Raman modes found in crystalline Li_2SO_4 ,¹³ which are marked as bars in the figure. The modes at 1123 and 1127 cm^{-1} in the crystal [appearing as a single bar in Figs. 1(a) and 1(b) due to their small separation], as well as the mode at 1194 cm^{-1} , seem to be shifted to higher frequencies and can be related to the bands around 1150 and 1225 cm^{-1} . Similarly, the two bands in the film around 415 and 645 cm^{-1} have likely their origin in the pair of modes at 447 and 513 cm^{-1} , and 617 and 665 cm^{-1} in the crystal, respectively.

The most intense line in the Raman spectrum of the crystal is the symmetric breathing mode of SO_4^{2-} at 1014 cm^{-1} , which in the glassy film is either very weak or shifted to the main band appearing at lower frequencies. That the main band in the glassy film covers a range of 850–1000 cm^{-1} without corresponding modes from the crystal suggests that it is associated with vibrational modes involving nitrogen. To test this presumption, it would be desirable to compare the data with those of a film sputtered from a Li_2SO_4 target in a nitrogen-free atmosphere. However, as discussed in the Introduction, such films cannot be grown, since the nitrogen

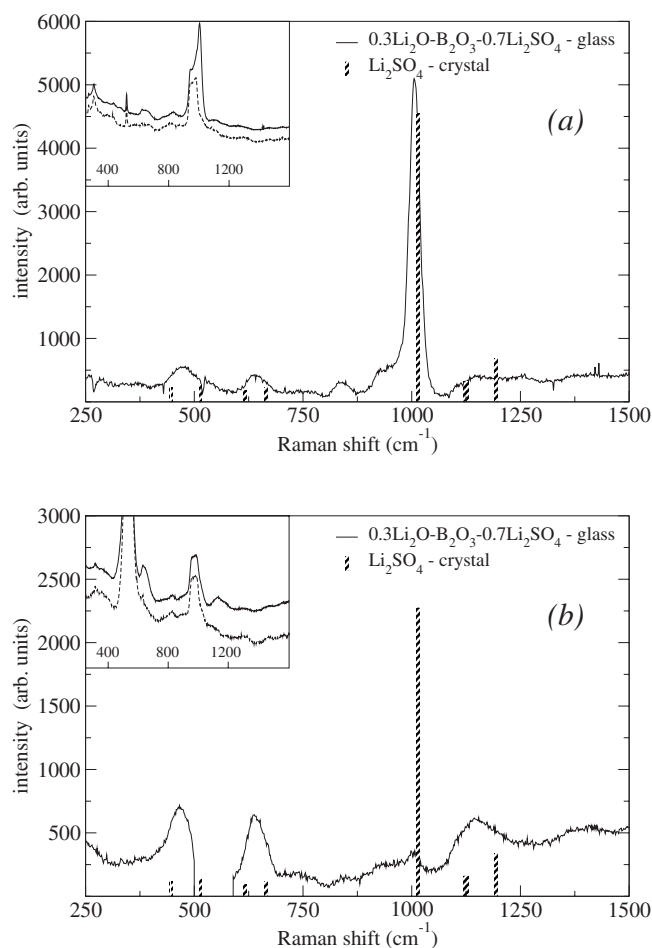


FIG. 2. (a) Polarized and (b) depolarized difference Raman spectra of films on a silicon substrate, which were sputtered from a $0.7\text{Li}_2\text{SO}_4\text{-}0.3\text{LiBO}_2$ target in an argon atmosphere. As in Fig. 1, the difference signal is obtained by subtracting the spectrum of a bare silicon substrate from the spectrum of the sample. The insets show the raw data from the sample and the substrate (dashed lines, silicon; solid lines, film sample). The spectra have been offset for clarity.

plays a crucial role in the glass forming ability. We therefore investigated a glassy film sputtered from a $0.7\text{Li}_2\text{SO}_4\text{-}0.3\text{LiBO}_2$ target in an argon atmosphere. The results for the polarized Raman spectrum shown in Fig. 2(a) clearly reveal that the main band seen in Fig. 1(a) is missing and only a broadened peak associated with the symmetric breathing mode of SO_4^{2-} appears. Moreover, as expected for a totally symmetric mode, this large peak is absent in the depolarized spectrum shown in Fig. 2(b). It also demonstrates that the main band seen in the LISON film in Fig. 1 cannot be associated with spurious contributions from the silicon substrate, giving confidence to the subtraction procedure.

V. THEORETICAL RESULTS AND COMPARISON WITH THE EXPERIMENT

For the comparison of the experiment with the calculated spectra, we will exclusively use the polarized Raman spec-

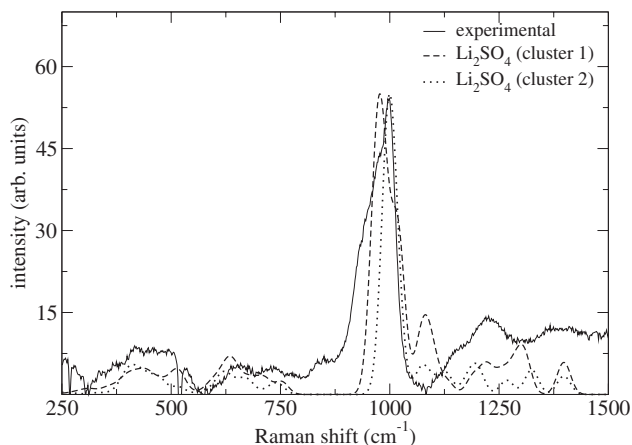


FIG. 3. Comparison of two calculated Raman spectra for Li_2SO_4 clusters with the experimental Raman data.

trum shown in Fig. 1(a), since it is not disturbed by the silicon mode at 521 cm^{-1} . To obtain a smooth spectrum from the calculated Raman lines, each line j with Raman shift ω_j and intensity I_j is replaced by a Gaussian peak function $I_j \exp[-(\omega - \omega_j)^2 / \Delta^2]$, with $\Delta = 20\text{ cm}^{-1}$.

In addition, a rescaling of the calculated Raman shifts is, in general, necessary to obtain good agreement with the experimental spectra, depending on the particular material and method used. Commonly used literature data for these rescaling factors exist for some gas and organic molecules. They have been determined by adjusting calculated to measured frequencies for well defined modes. In our case, such literature data are not available and we have to determine the rescaling factor by other means. To do this, we focus on the SO_4 breathing mode of the crystal, since one should expect it to be present also in the clusters and the film (possibly with reduced intensity). The calculated SO_4 breathing mode frequencies differ slightly from each other due to the different local surroundings of the SO_4^{2-} anions in the clusters. Taking the average of them and determining the quotient with the corresponding crystal mode frequency give a stretching factor of 1.11. Using this factor yields theoretical spectra which appear to be shifted to higher frequencies. An optimal overlap of calculated and measured spectra is obtained with a slightly reduced factor of 1.09. This minor correction should not be surprising as some shift of the breathing mode frequency can be expected when considering the crystal and the film. To summarize, for the comparison, the frequencies of all calculated spectra are stretched by this factor of 1.09.

A. Li_2SO_4 clusters

Figure 3 shows the Raman spectra calculated from two optimized Li_2SO_4 cluster configurations (dotted and dashed lines) in comparison with the measured Raman spectrum (solid line). As can be seen from the figure, the calculated spectra for the two different optimized clusters do not deviate much. This can be interpreted in the way that local arrangements participating in the dominating vibrations are determined by the Li^+ and SO_4^{2-} ions and their mutual

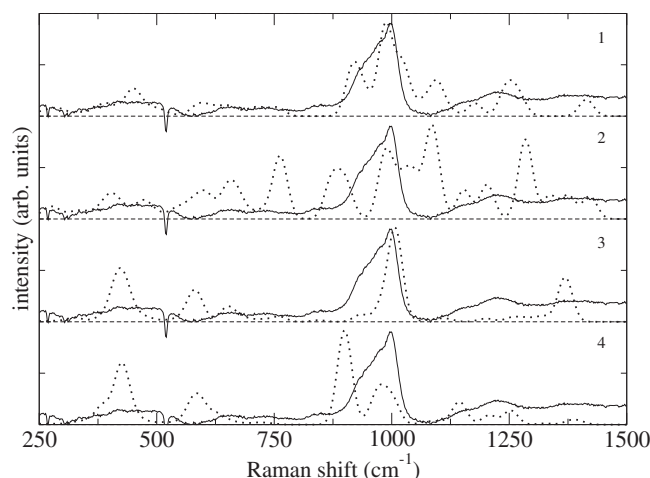


FIG. 4. Comparison of four calculated Raman spectra (dotted lines) for LISON clusters with the experimental Raman data (solid lines).

Coulomb interaction as in the crystal. As a consequence, the SO_4^{2-} units are rather weakly coupled.

In comparison to the measured Raman spectrum, the calculated ones resemble the overall band structure. However, there are two important differences. (i) The experimental spectrum shows the main band between 850 and 1000 cm^{-1} . As there exists not a single vibrational mode between 760 and 960 cm^{-1} , this band is absent in the calculated spectra. (ii) In the calculated spectra, there is intensity due to a mode at 1080 cm^{-1} , while almost no intensity is seen around this frequency in the experimental spectrum. As a first hypothesis, deviation (ii) can be related to the finite size of the calculated cluster. A closer inspection of the eigenvector belonging to this mode reveals that it contains an oxygen atom, which moves in the normal direction of the surface of the cluster. Accordingly, this mode can be attributed to an artifact of the limited cluster size.

Deviation (i), on the other hand, may be due to structural changes when nitrogen is incorporated in the structure, which can be investigated by comparing experimental spectra to calculated spectra from the nitrogen containing clusters.

B. $\text{Li}_2\text{SO}_4\text{-N}$ clusters

The substitution of two oxygen atoms by nitrogen atoms in a cluster has a strong effect on the calculated spectra, as can be seen from Fig. 4, where spectra of four different clusters (labeled 1–4 in the figure) are compared to the measured Raman spectrum. This is not surprising as half of the SO_4^{2-} are replaced by SO_3N^{3-} . The rather large amount of nitrogen corresponds to results from the Rutherford backscattering experiments which yielded a ratio of about 2:1 of sulfur to nitrogen¹⁷ and are also in agreement with previously reported values.⁶

A number of new bands appear in the calculated spectra from the nitrogen containing clusters. However, while the clusters without nitrogen lead to very similar spectra, the

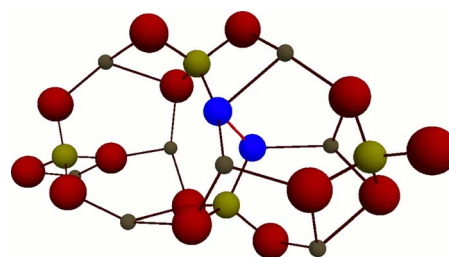


FIG. 5. (Color online) Atomic configuration of the optimal LISON cluster (corresponding to spectrum 1 in Fig. 4). Oxygen atoms are marked in red (dark gray, large spheres), sulfur atoms in yellow (light gray, midsize spheres), nitrogen atoms in blue (dark gray, midsize spheres), and lithium atoms in silver (gray, small spheres).

modified systems show pronounced differences. In general, spectra 2–4 do not compare well with the experimental data, while calculated spectrum 1 is surprisingly close to the experimental one. In particular, the main band here is well reproduced. The additional band at 1080 cm^{-1} is still present, but it does not relate to nitrogen incorporation as discussed above. It is interesting to note that optimal cluster 1 does not only compare most favorably with the experimental spectrum but also has the lowest energy (1.9 eV lower than the next lowest energy, which belongs to the cluster with spectrum 3).

Figure 5 shows the atomic configuration of optimal cluster 1. In contrast to clusters 2–4, it contains an interaction between two nitrogen atoms in close proximity at a distance of 1.47 Å, which serves as a type of bridge between the two SO_3N pseudotetrahedra. This suggests that the incorporation of nitrogen triggers the formation of structures, which, by hindering a reorientation of the anions relative to each other, prevent the crystallization of the film (or, more precisely, increases the free energy barrier for crystallization).

The reason for the formation of the N-N bridges could be a compensation of the higher valence (−3) of nitrogen compared to −2 of oxygen. One can speculate that additional lithium compensates for this valence difference in the film. To test if the N-N bridges also form in this case, we have performed additional electronic structure calculations, where for each nitrogen atom an additional lithium atom was introduced. Indeed, the N-N bridges also form in this situation, which gives further support for the proposed mechanism of glass stabilization.

VI. CONCLUSIONS

By comparing experimental and calculated Raman spectra for LISON systems, we are able to show that a good representation of an amorphous LISON film is possible using small atomic clusters. Our investigations reveal that in the LISON structure, nitrogen is replacing oxygen in the SO_4^{2-} tetrahedra. In the configuration yielding Raman spectra in agreement with the experiments, we find a nitrogen-nitrogen bridge between two anions. This suggests that this bridge formation is the underlying reason for the prevention of crystallization of the LISON material during the sputtering pro-

cess. The bridges can restrain the reorientation of the anions and stabilize an amorphous film structure.

ACKNOWLEDGMENTS

We thank Yohann Hamon and Philippe Vinatier from École Nationale Supérieure de Chimie et Physique de Bor-

deaux, France, for providing the LISON samples, and Efstratios Kamitsos from the Theoretical and Physical Chemistry Institute of the National Hellenic Research Foundation, Athens, Greece, for valuable discussions. Financial support by the HI-CONDELEC EU STREP project (NMP3-CT-2005-516975) is gratefully acknowledged.

*philipp.maass@tu-ilmenau.de; URL: <http://www.tu-ilmenau.de/theophys2>

¹X. Yu, J. B. Bates, G. E. Ellison, Jr., and F. X. Hart, *J. Electrochem. Soc.* **144**, 524 (1997).

²Y. S. Park, S. H. Lee, B. I. Lee, and S. K. Joo, *Electrochem. Solid-State Lett.* **2**, 58 (1999).

³A. Gerouki and R. Goldner, *Solid-State Ionics V*, MRS Symposia Proceedings No. 548 (Materials Research Society, Pittsburgh, 1999), p. 679.

⁴S. J. Lee, A. K. Baik, and S. M. Lee, *Electrochem. Commun.* **5**, 32 (2003).

⁵K. H. Joo, P. Vinatier, B. Pecquenard, A. Levasseur, and H. J. Sohn, *Solid State Ionics* **160**, 51 (2003).

⁶K. H. Joo, H. J. Sohn, P. Vinatier, B. Pecquenard, and A. Levasseur, *Electrochem. Solid-State Lett.* **7**, A256 (2004).

⁷N. Hellgren, M. P. Johansson, E. Broitman, L. Hultman, and J.-E. Sundgren, *Phys. Rev. B* **59**, 5162 (1999).

⁸D. Roy, M. Chhowalla, N. Hellgren, T. W. Clyne, and G. A. J. Amaratunga, *Phys. Rev. B* **70**, 035406 (2004).

⁹N. K. Cuong, M. Tahara, N. Yamauchi, and T. Sone, *Surf. Coat. Technol.* **193**, 283 (2005).

¹⁰P. B. Leezenberg, W. H. Johnston, and G. W. Tyndall, *J. Appl. Phys.* **89**, 3498 (2001).

¹¹R. Gupta and M. Gupta, *Phys. Rev. B* **72**, 024202 (2005).

¹²The sample was prepared at École Nationale Supérieure de Chimie et Physique de Bordeaux.

¹³E. Cazzanelli and R. Frech, *J. Chem. Phys.* **79**, 2615 (1983); **81**, 4729 (1984). Only the modes belonging to the A_g symmetry are

considered (other representations have slightly shifted modes, but the sizes of the corresponding shifts are negligible in comparison with the width of the peaks obtained for the film).

¹⁴R. Dennington II, T. Keith, J. Millam, K. Eppinnett, W. L. Hovell, and R. Gilliland, *GAUSSVIEW*, Version 3.09, Semichem, Inc., Shawnee Mission, KS, 2003.

¹⁵M. J. Frisch, G. W. Trucks, H. B. Schlegel, G. E. Scuseria, M. A. Robb, J. R. Cheeseman, J. A. Montgomery, Jr., T. Vreven, K. N. Kudin, J. C. Burant, J. M. Millam, S. S. Iyengar, J. Tomasi, V. Barone, B. Mennucci, M. Cossi, G. Scalmani, N. Rega, G. A. Petersson, H. Nakatsuji, M. Hada, M. Ehara, K. Toyota, R. Fukuda, J. Hasegawa, M. Ishida, T. Nakajima, Y. Honda, O. Kitao, H. Nakai, M. Klene, X. Li, J. E. Knox, H. P. Hratchian, J. B. Cross, V. Bakken, C. Adamo, J. Jaramillo, R. Gomperts, R. E. Stratmann, O. Yazyev, A. J. Austin, R. Cammi, C. Pomelli, J. W. Ochterski, P. Y. Ayala, K. Morokuma, G. A. Voth, P. Salvador, J. J. Dannenberg, V. G. Zakrzewski, S. Dapprich, A. D. Daniels, M. C. Strain, O. Farkas, D. K. Malick, A. D. Rabuck, K. Raghavachari, J. B. Foresman, J. V. Ortiz, Q. Cui, A. G. Baboul, S. Clifford, J. Cioslowski, B. B. Stefanov, G. Liu, A. Liashenko, P. Piskorz, I. Komaromi, R. L. Martin, D. J. Fox, T. Keith, M. A. Al-Laham, C. Y. Peng, A. Nanayakkara, M. Challacombe, P. M. W. Gill, B. Johnson, W. Chen, M. W. Wong, C. Gonzalez, and J. A. Pople, *GAUSSIAN 03*, Revision C.02, Gaussian, Inc., Wallingford, CT, 2004.

¹⁶C. J. Cramer, *Essentials of Computational Chemistry* (Wiley, New Jersey, 2004).

¹⁷Y. Hamon and P. Vinatier (private communication).